Supporting Information

Ratiometric Dual-Emitting Thermometers Based on Rhodamine B Dye-Incorporated (Nano) Curcumin Periodic Mesoporous Organosilicas for Bioapplications

Chunhui Liu[a,b,c], Simona Premcheska[c,d], Andre Skirtach[d], Dirk Poelman[b], Anna M. Kaczmarek[c], and Pascal Van Der Voort[a]**

[a]COMOC - Center for Ordered Materials Organometallics and Catalysis, Department of Chemistry, Ghent University, Krijgslaan 281 S3, 9000 Ghent;
[b]Lumilab, Department of Solid State Sciences, Ghent University, Krijgslaan 281 S1, 9000 Ghent;
[c]NanoSensing Group, Department of Chemistry, Ghent University, Krijgslaan 281 S3, 9000 Ghent
[d]
** Corresponding authors: Email: Anna.Kaczmarek@Ugent.be ；Email: Pascal.VanDerVoort@UGent.be*

Table S1 Preparation of PMO@dye.

Material (x=)	C-PMO@RhBx@LB		CP-PMO@RhBx@LB	
	Rhb (mg)	Water (mL)	Rhb (mg)	Water (mL)
1	0.1	2	0.1	2
2	0.1	4	0.1	10
3	0.1	10	0.1	20
4	0.1	20		

Table S2 Fitting parameters of prepared C-PMO and CP-PMO.

Material	Δ_0	α	ΔE (cm^{-1})
C-PMO@RhB3@LB	3.47	$3.13*10^5$	3065.4
CP-PMO@RhB1@LB	0.41	$5.89*10^5$	2936.5

Δ_0 is the thermometric parameter at T = 0 K.; $\alpha = W_0/W_R$ is the ratio between the nonradiative rates (W_0 is at T = 0 K) and radiative rates (W_R); ΔE is the activation energy of the nonradiative process.

Table S3. Comparison to the maximum relative sensitivities of several previously reported luminescent host-guest MOFs for temperature sensing.

Materials	Temperature range	Max S_r	T_m	Ref.
DSM@ZnPZDDI	298-338 K	0.44 %·K^{-1}	298 K	5
DSM@ZJU-56	298-343 K	1.11 %·K^{-1}	298 K	
Rh101@UiO-67	293-333 K	1.30 %·K^{-1}	333 K	6
ZJU-88⊃perylene	293-353 K	1.28 %·K^{-1}	293 K	7
TbTATAB⊃C460	100-300 K	4.484 %·K^{-1}	300 K	8
$CsPbBr_3$@Eu-BTC	20-100 °C (293-373 K)	3.9 %·K^{-1}	20 °C (293 K)	9
RhB@IRMOF-3	20-70 °C (293-343 K)	0.87 %·K^{-1}	70 °C (343 K)	10
FL@IRMOF-3	20-80 °C (293-353 K)	0.66 %·K^{-1}	80 °C (353 K)	
$Dye_{0.01}$@Eu-BTC		0.50 %·K^{-1}	363 K	
$Dye_{0.005}$@Eu-BTC	283-363 K	0.45 %·K^{-1}	363 K	11
$Dye_{0.001}$@Eu-BTC		0.30 %·K^{-1}	363 K	
RhB@ZnNDPA	30-90 °C (303-363 K)	0.42 %·K^{-1}	30 °C (303 K)	12
ZJU-21⊃DMASM	20-80 °C (293-353 K)	5.20%·K^{-1}	20 °C (293 K)	13
C-PMO@RhB@LB	293-343 K	1.69%·K^{-1}	343 K	This work
CP-PMO@RhB@LB	293-343 K	2.60%·K^{-1}	343 K	

Sr is relative sensitivity; T_m is temperature when S_r is maximum.

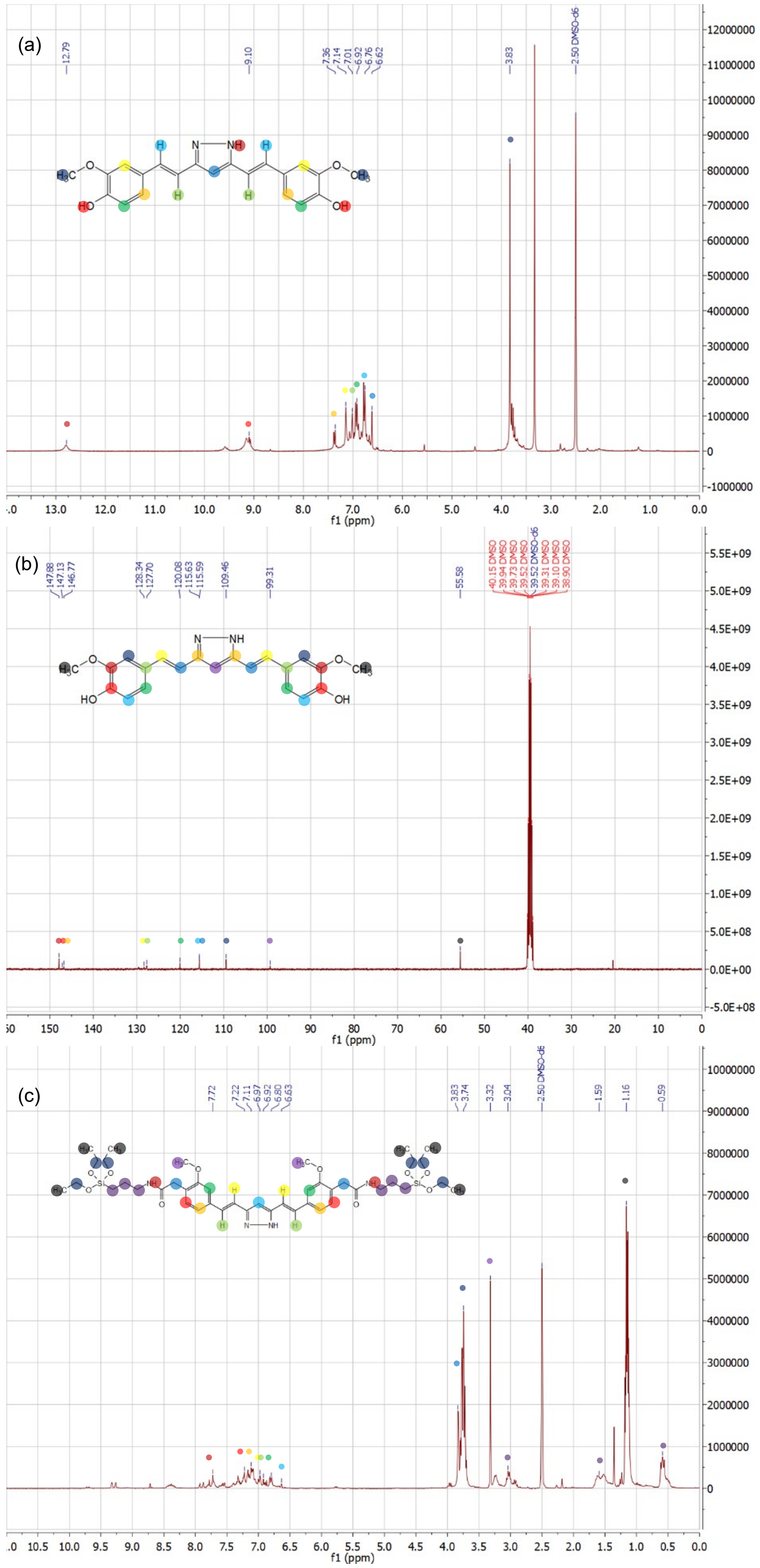
(a)
12.79
9.10
7.36
7.14
7.01
6.92
6.76
6.62
3.83
2.50 DMSO-d6
f1 (ppm)
(b)
147.88
147.13
146.77
128.34
127.70
120.08
115.63
115.59
109.46
99.31
55.58
40.15 DMSO
39.94 DMSO
39.73 DMSO
39.52 DMSO
39.52 DMSO-d6
39.31 DMSO
39.10 DMSO
38.90 DMSO
f1 (ppm)
(c)
7.72
7.22
7.11
6.97
6.92
6.80
6.63
3.83
3.74
3.32
3.04
2.50 DMSO-d6
1.59
1.16
0.59
f1 (ppm)

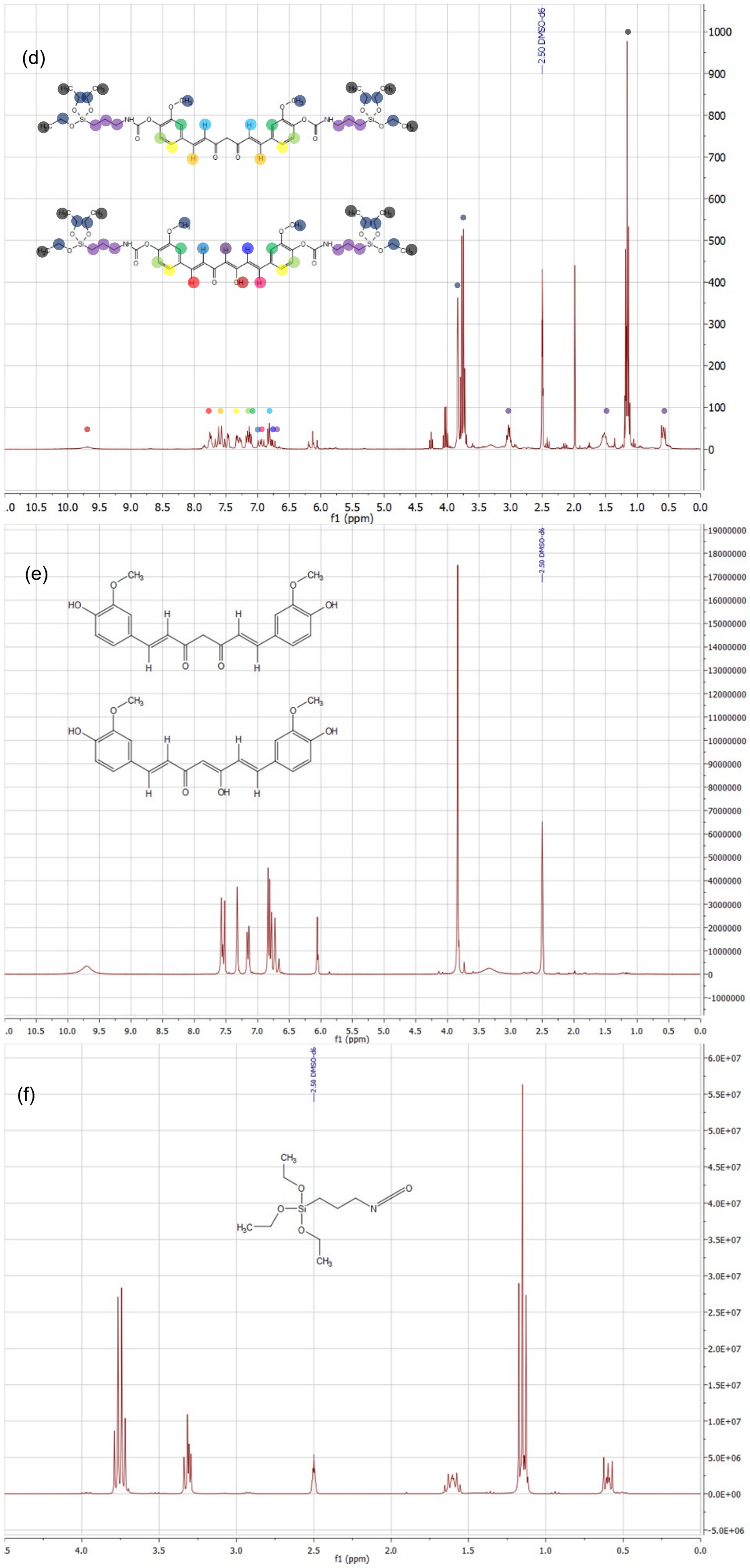

Figure S 1 ^{1}H NMR of (a) curcumin-pyrazole analog, 1c; ; (c) curcumin-pyrazole-Si, 1d; (d) curcumin- Si, 1b (e)curcumin, 1a; (f) (3-Isocyanatopropyl) triethoxysilane (IPTES), and ^{13}C NMR of (b) curcumin-pyrazole analog, 1c.

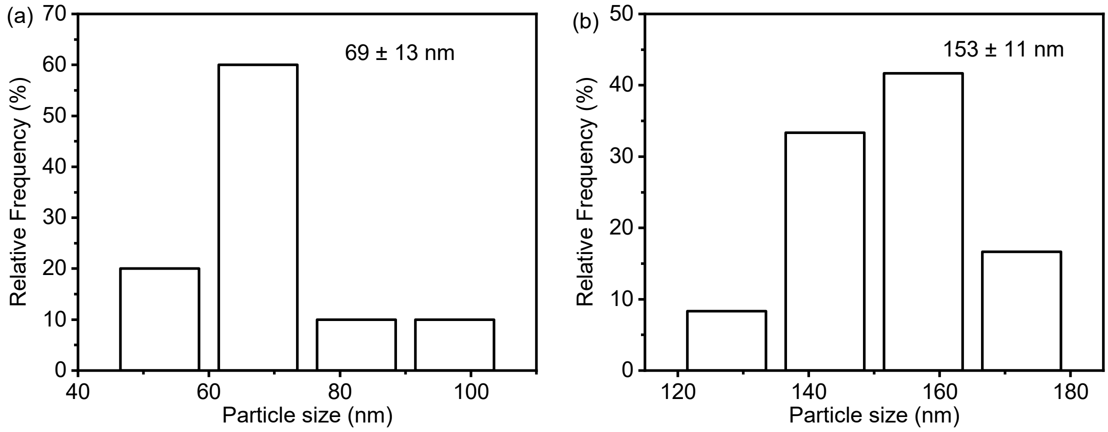

Figure S 2 Histograms showing the particle size distribution of: (a) C-PMO; (b) CP-PMO. The particle size is based on collected TEM images.

Figure S 3 Photograph of the prepared PMO@RhB@LB samples at (a) daylight (up) and when placed under a laboratory UV lamp with an excitation wavelength of 365 nm (down); (b) 293 K (20 ^{o}C) in water (up), and 343 K (70 ^{o}C) in water (down) under a laboratory UV lamp of 365 nm excitation.

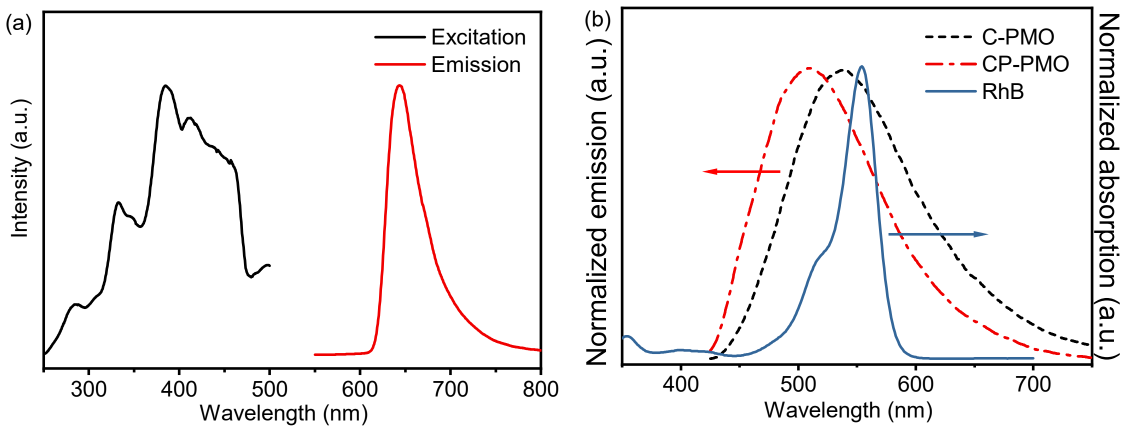

Figure S 4 (a) Excitation and emission spectra of RhB in water at room temperature (excited at 417 nm observed at 641 nm). (b) Emission spectra of the two PMOs – C-PMO AND CP-PMO (excited at 417 nm) and UV-vis absorption spectrum of RhB in water at room temperature.

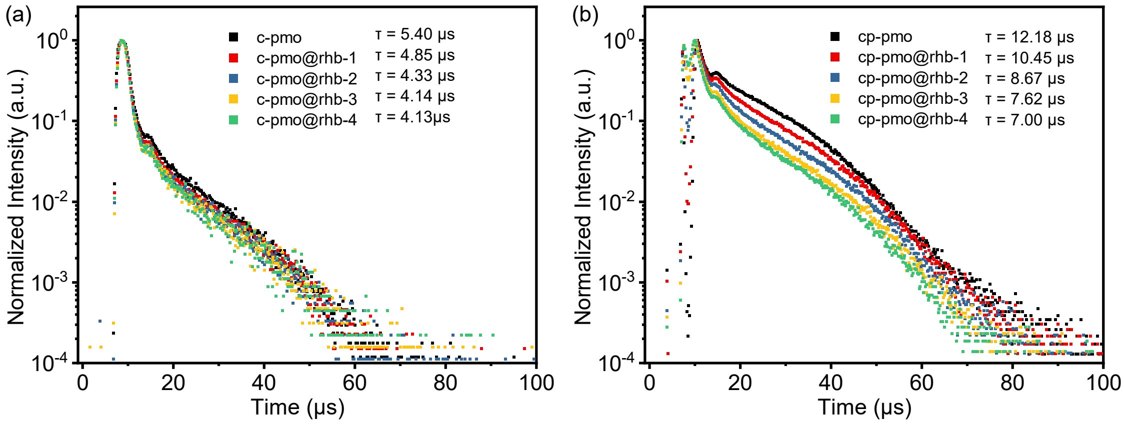

(a)
c-pmo τ = 5.40 μs
c-pmo@rhb-1 τ = 4.85 μs
c-pmo@rhb-2 τ = 4.33 μs
c-pmo@rhb-3 τ = 4.14 μs
c-pmo@rhb-4 τ = 4.13μs
Normalized Intensity (a.u.)
Time (μs)
(b)
cp-pmo τ = 12.18 μs
cp-pmo@rhb-1 τ = 10.45 μs
cp-pmo@rhb-2 τ = 8.67 μs
cp-pmo@rhb-3 τ = 7.62 μs
cp-pmo@rhb-4 τ = 7.00 μs
Normalized Intensity (a.u.)
Time (μs)

Figure S 5 Luminescence decay profiles of (a)C-PMO, and (b) CP-PMO in water upon added increasing concentrations of RhB water solution, ex = 417 nm, em = 525 nm (τ: average decay time).

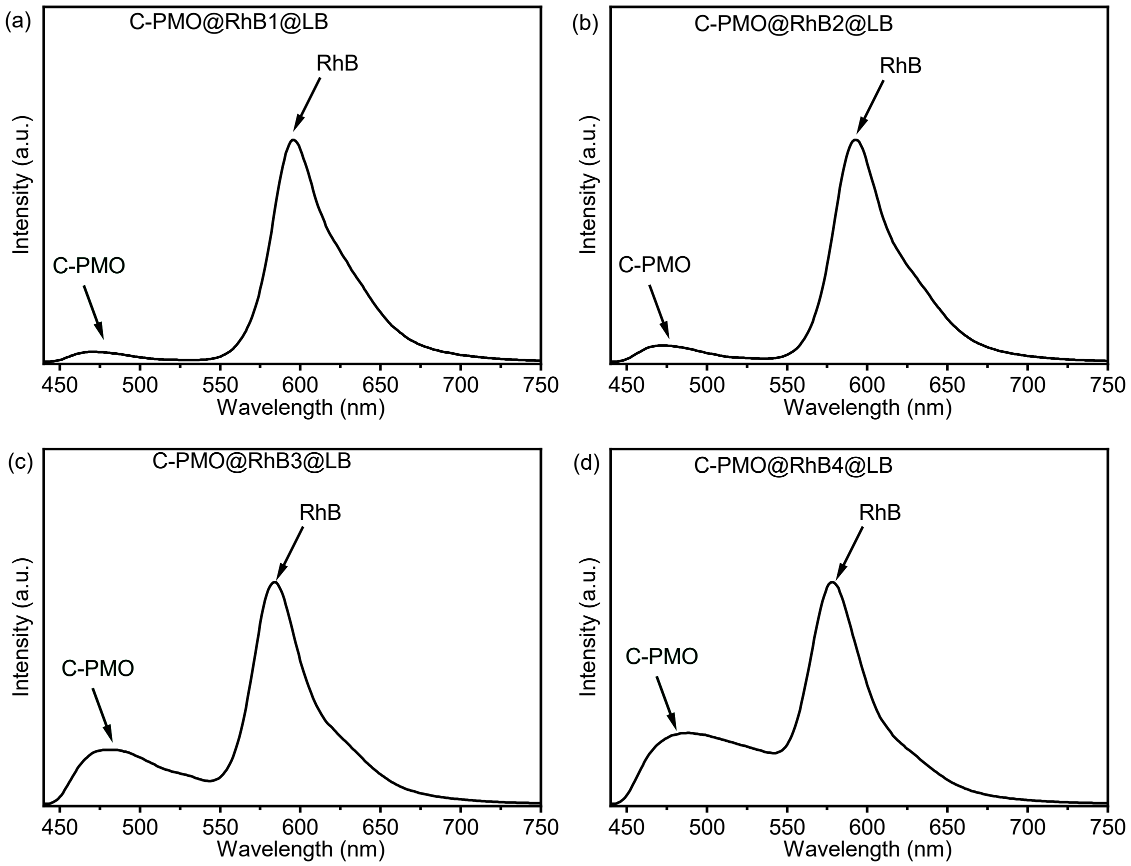

Figure S 6 Emission spectra of C-PMO@RhB with different dye contents in water excited at 417 nm.

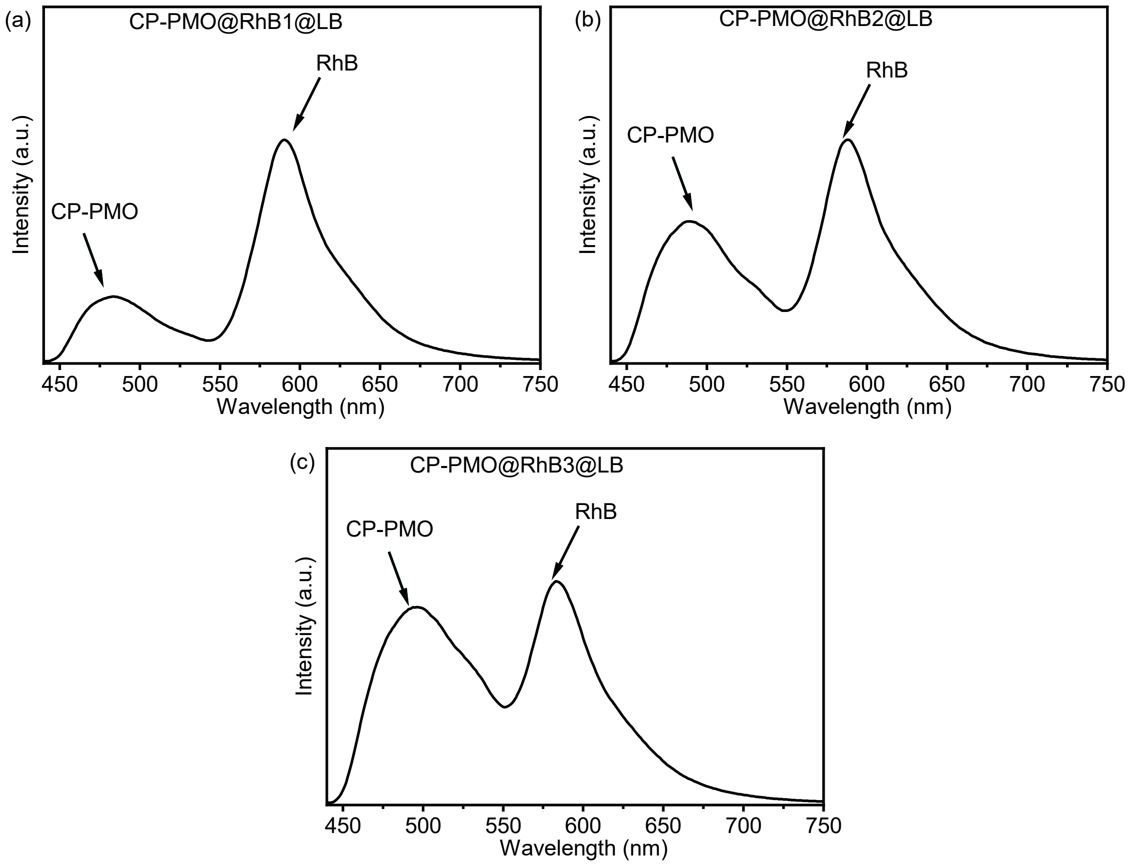

Figure S 7 Emission spectra of CP-PMO@RhB with different dye contents in water excited at 417 nm.

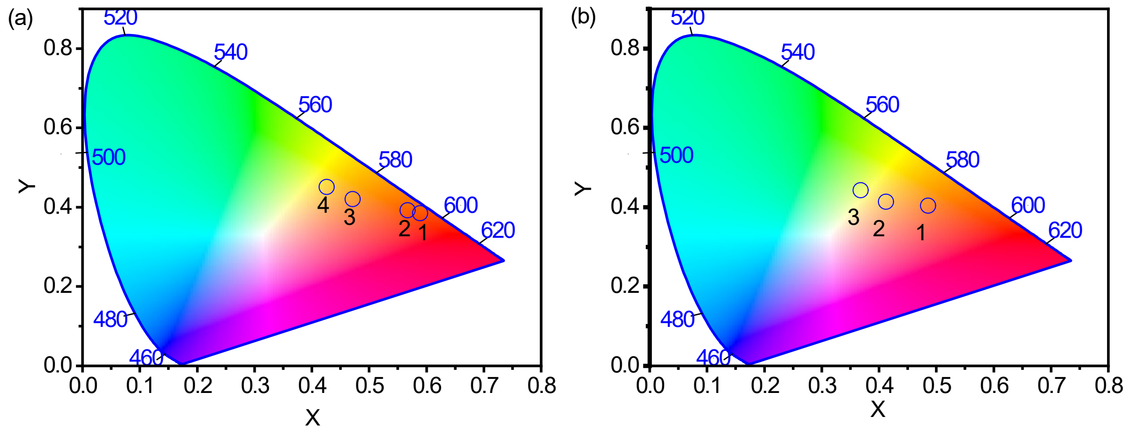

Figure S 8 CIE chromaticity diagram for (a)C-PMO@RhBx@LB (x=1~4) and (b) C-PMO@RhBx@LB (x=1~3) with decreasing dye contents excited at 417 nm.

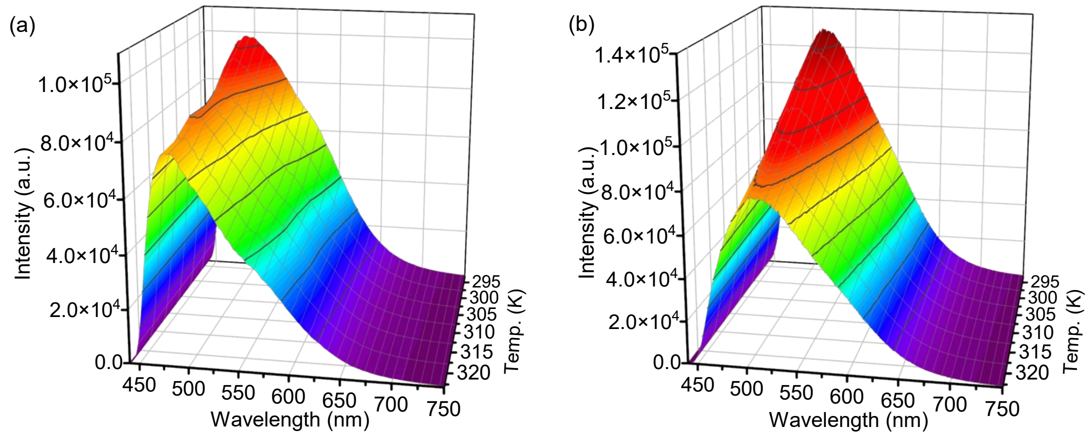

Figure S 9 Temperature-dependent emission spectra of (a) C-PMO and (b)CP-PMO dispersed in water recorded from 293.15 to 323.15 K, excited at 417 nm.

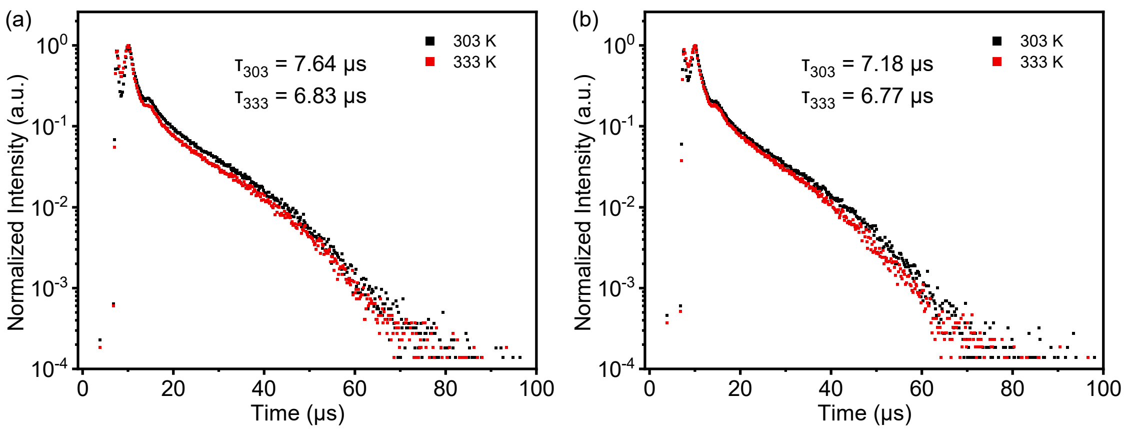

Figure S 10 Luminescence decay profile of (a)C-PMO in water, ex = 417 nm, em = 539 nm; (b) CP-PMO in water, ex = 417 nm, em = 533 nm.

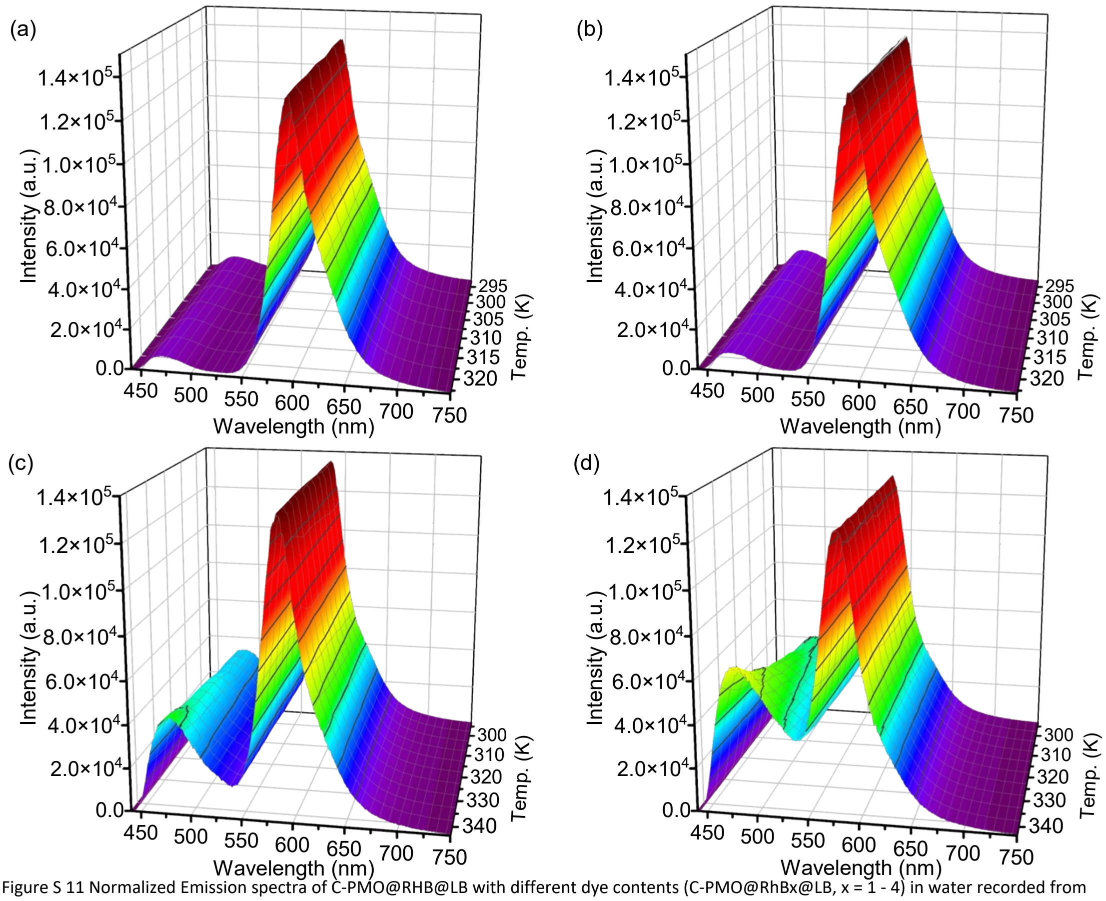

Figure S 11 Normalized Emission spectra of C-PMO@RHB@LB with different dye contents (C-PMO@RhBx@LB, x = 1 - 4) in water recorded from 293.15 to 343.15 K, excited at 417 nm.

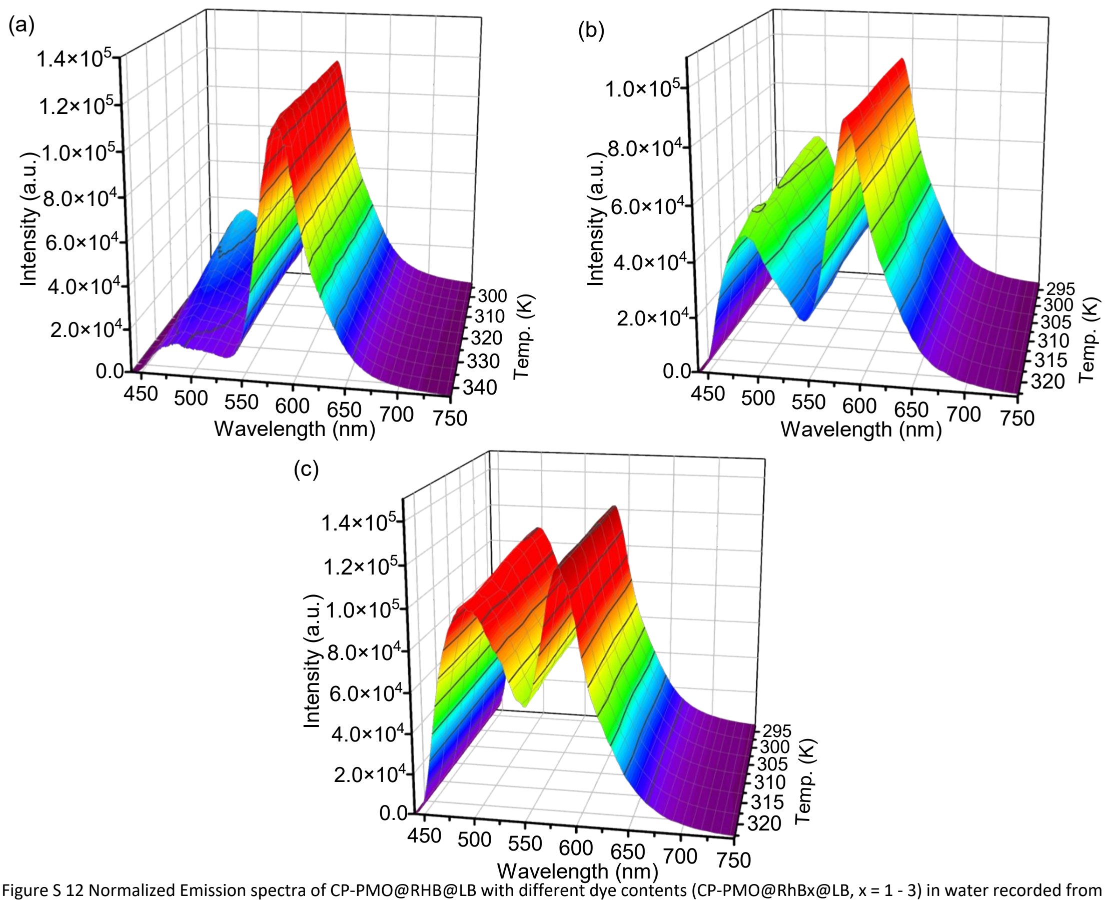

Figure S 12 Normalized Emission spectra of CP-PMO@RHB@LB with different dye contents (CP-PMO@RhBx@LB, x = 1 - 3) in water recorded from 293.15 to 343.15 K, excited at 417 nm.

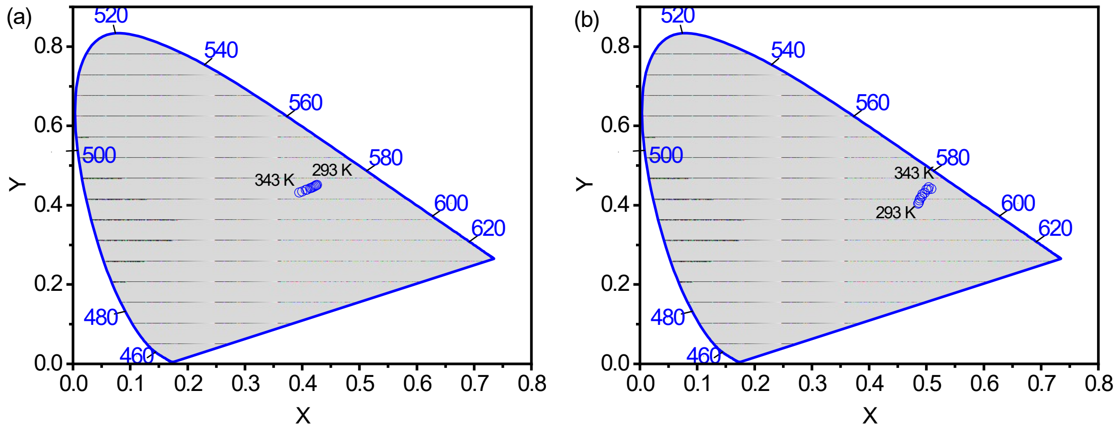

(a)
520
540
560
580
600
620
500
480
460
343 K
293 K
Y
X
(b)
520
540
560
580
600
620
500
480
460
343 K
293 K
Y
X

a

Figure S 13 CIE coordinates diagram for (a) C-PMO@RhB@LB; (b) CP-PMO@RhB@LB at different temperatures (293–343 K).

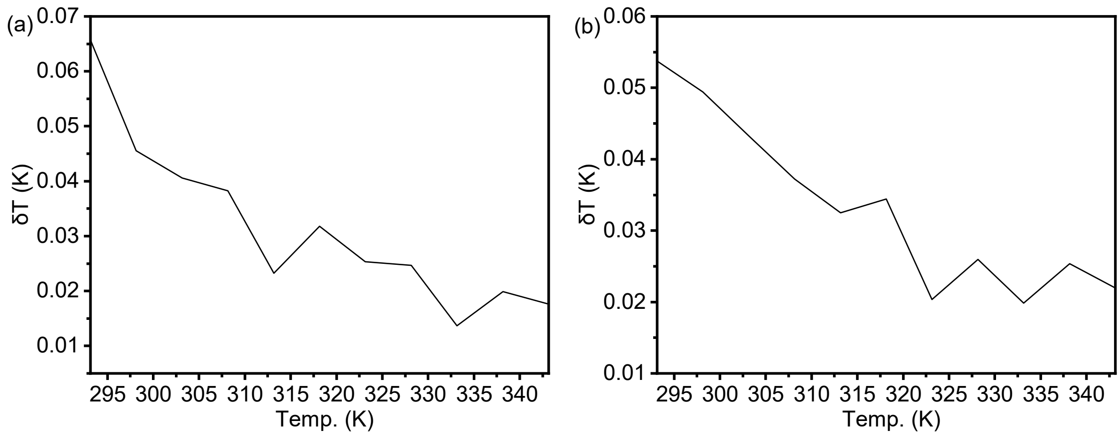

Figure S 14 Temperature uncertainty for (a) C-PMO@RhB@LB; (b) CP-PMO@RhB@LB at varying temperatures (293-343 K).

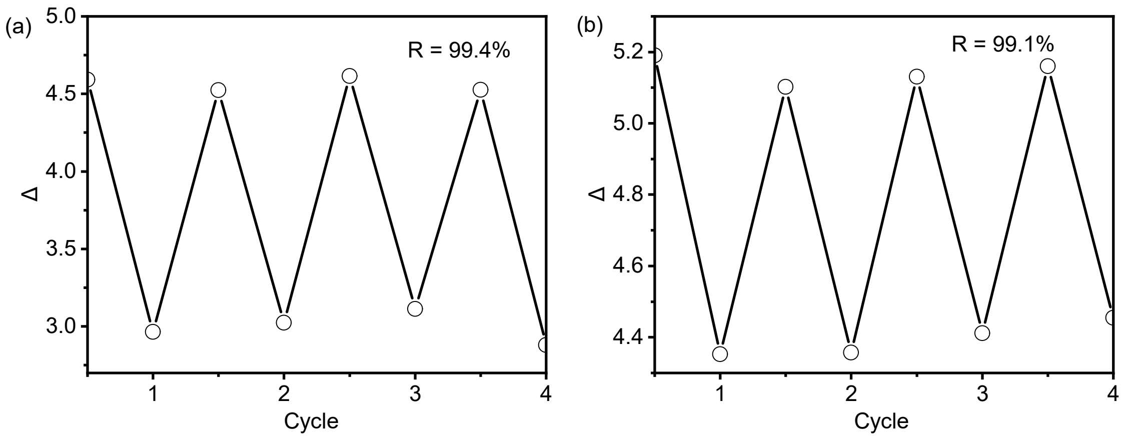

(a)
R = 99.4%
Δ
Cycle
5.0
4.5
4.0
3.5
3.0
1
2
3
4
(b)
R = 99.1%
Δ
Cycle
5.2
5.0
4.8
4.6
4.4
1
2
3
4

Figure S 15 Cycle tests for (a)C-PMO@RhB@LB, and (b) CP-PMO@RhB@LB (R - repeatability).

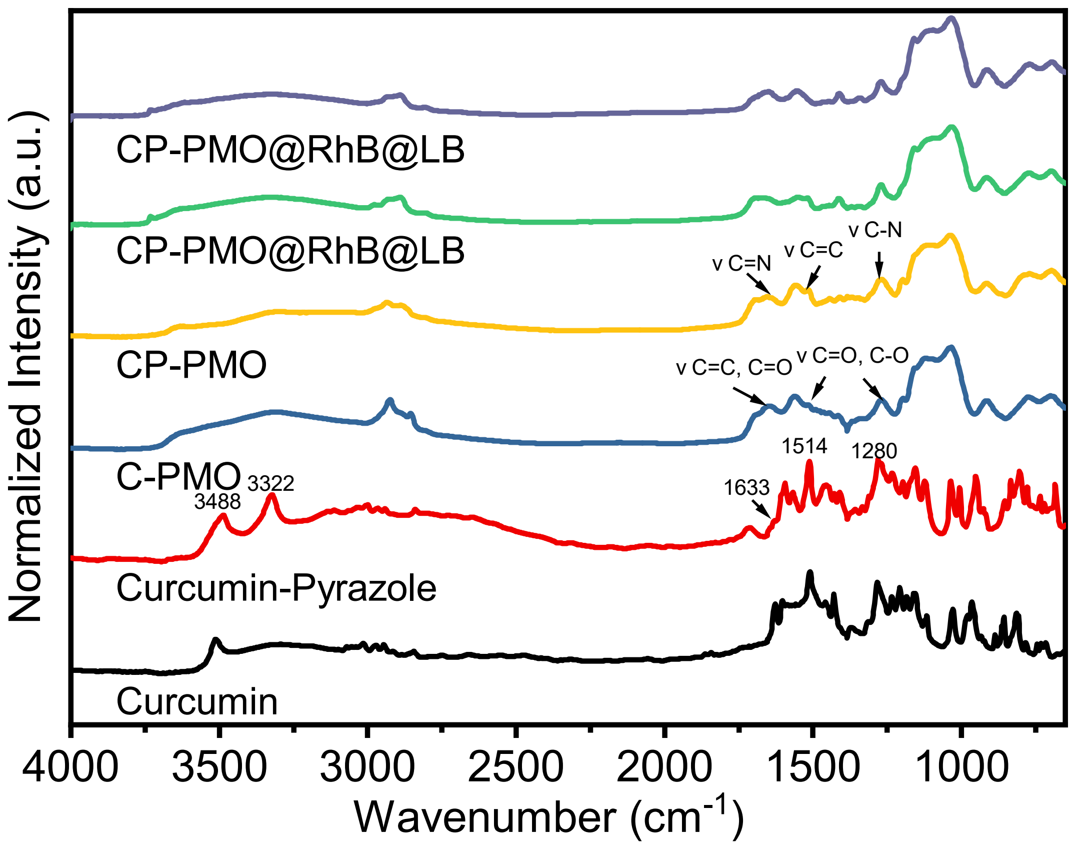

Figure S 16 FTIR spectra of PMO@RhB@LB.

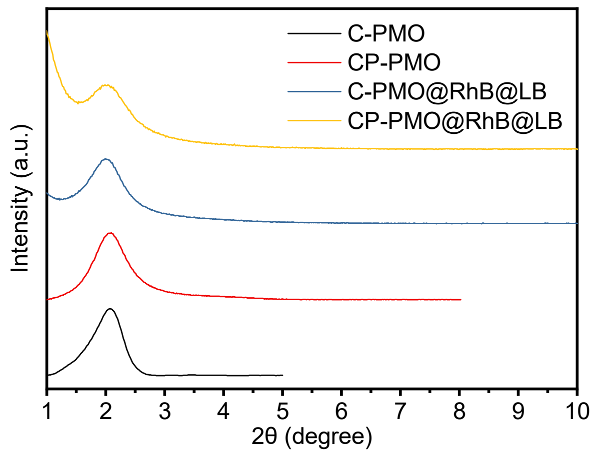

Figure S 17 PXRD patterns of PMOs@RhB@LB

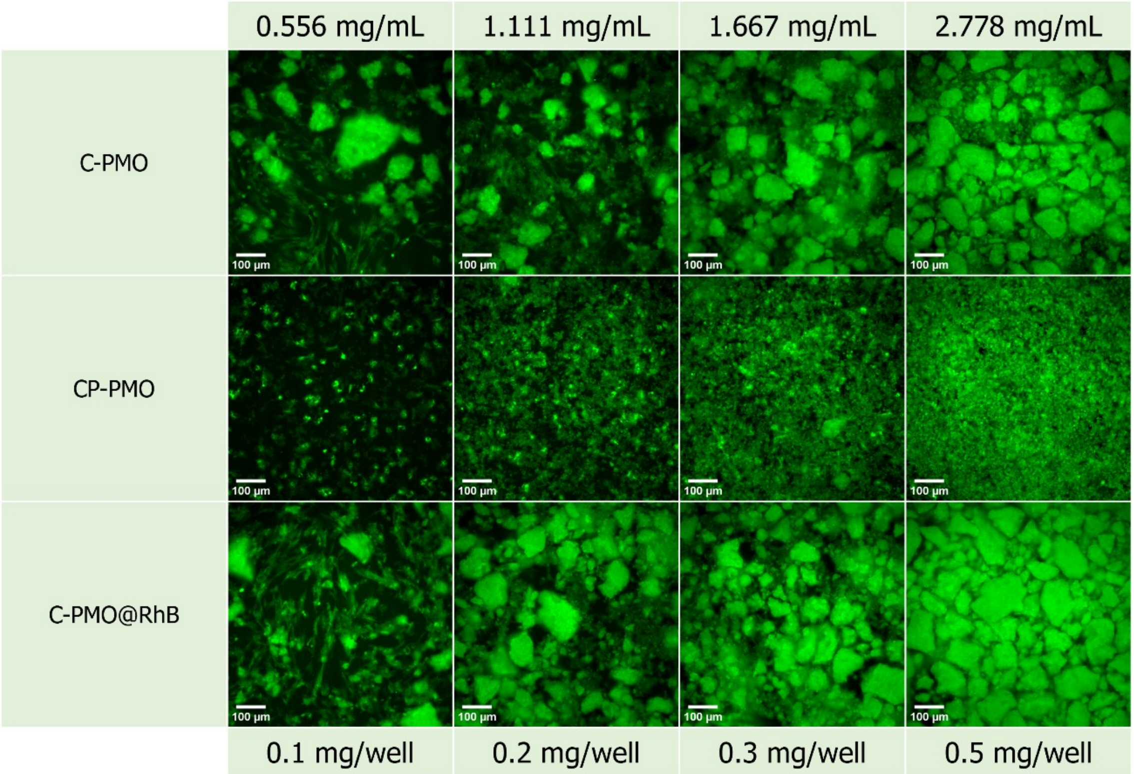

Figure S 18 Fluorescence microscopy images of the technical replicates with stained NHDF cells for the three samples (C-PMO, CP-PMO, C-PMO@RhB4@LB) in the range of 0.1-0.5 mg/well. Calcein-AM was used as the cell stain at a final well concentration of 1.5 µM. All scale bars are set to 100 µm.

References

1. A. M. Kaczmarek, R. Van Deun and M. K. Kaczmarek, *Sens. Actuators B Chem.*, 2018, **273**, 696-702.
2. S. Datz, H. Engelke, C. V. Schirnding, L. Nguyen and T. Bein, *Microporous Mesoporous Mater.*, 2016, **225**, 371-377.
3. N. Ahsan, S. Mishra, M. K. Jain, A. Surolia and S. Gupta, *Sci. Rep.*, 2015, **5**, 1-16.
4. H. Rijckaert, S. Premcheska, S. Mohanty, J. Verduijn, A. Skirtach and A. M. Kaczmarek, *Physica B Condens. Matter*, 2022, **626**, 413453.
5. S. Wang, M. Gong, X. Han, D. Zhao, J. Liu, Y. Lu, C. Li and B. Chen, *ACS Appl. Mater. Interfaces*, 2021, **13**, 11078-11088.
6. Y. Zhou, D. Zhang, J. Zeng, N. Gan and J. Cuan, *Talanta*, 2018, **181**, 410-415.
7. Y. Cui, R. Song, J. Yu, M. Liu, Z. Wang, C. Wu, Y. Yang, Z. Wang, B. Chen and G. Qian, *Adv. Mater.*, 2015, **27**, 1420-1425.
8. T. Xia, T. Song, Y. Cui, Y. Yang and G. Qian, *Dalton Trans.*, 2016, **45**, 18689-18695.
9. J. Liu, Y. Zhao, X. Li, J. Wu, Y. Han, X. Zhang and Y. Xu, *Cryst. Growth Des.*, 2019, **20**, 454-459.
10. C. He, H. Yu, J. Sun, C. Zhou, X. Li, Z.-M. Su, F. Liu and V. Khakhinov, *Dyes Pigm.*, 2022, **198**, 110000.
11. J. Liu, X. Yue, Z. Wang, X. Zhang and Y. Xu, *J Mater Chem C*, 2020, **8**, 13328-13335.
12. M. Y. Gong, Z. J. Li, W. Q. Xiang, T. F. Xia and D. Zhao, *J Solid State Chem*, 2022, **311**, 123147.
13. D. Zhao, D. Yue, K. Jiang, Y. Cui, Q. Zhang, Y. Yang and G. Qian, *J Mater Chem C*, 2017, **5**, 1607-1613.